ideon

WHITE PAPER

Muon Tomography Applied to Nickel Massive Sulphide Deposits

Doug Schouten, Erin Western, Matt Owers, Clayton Wright, Adebayo Ojo, and Nigel Phillips

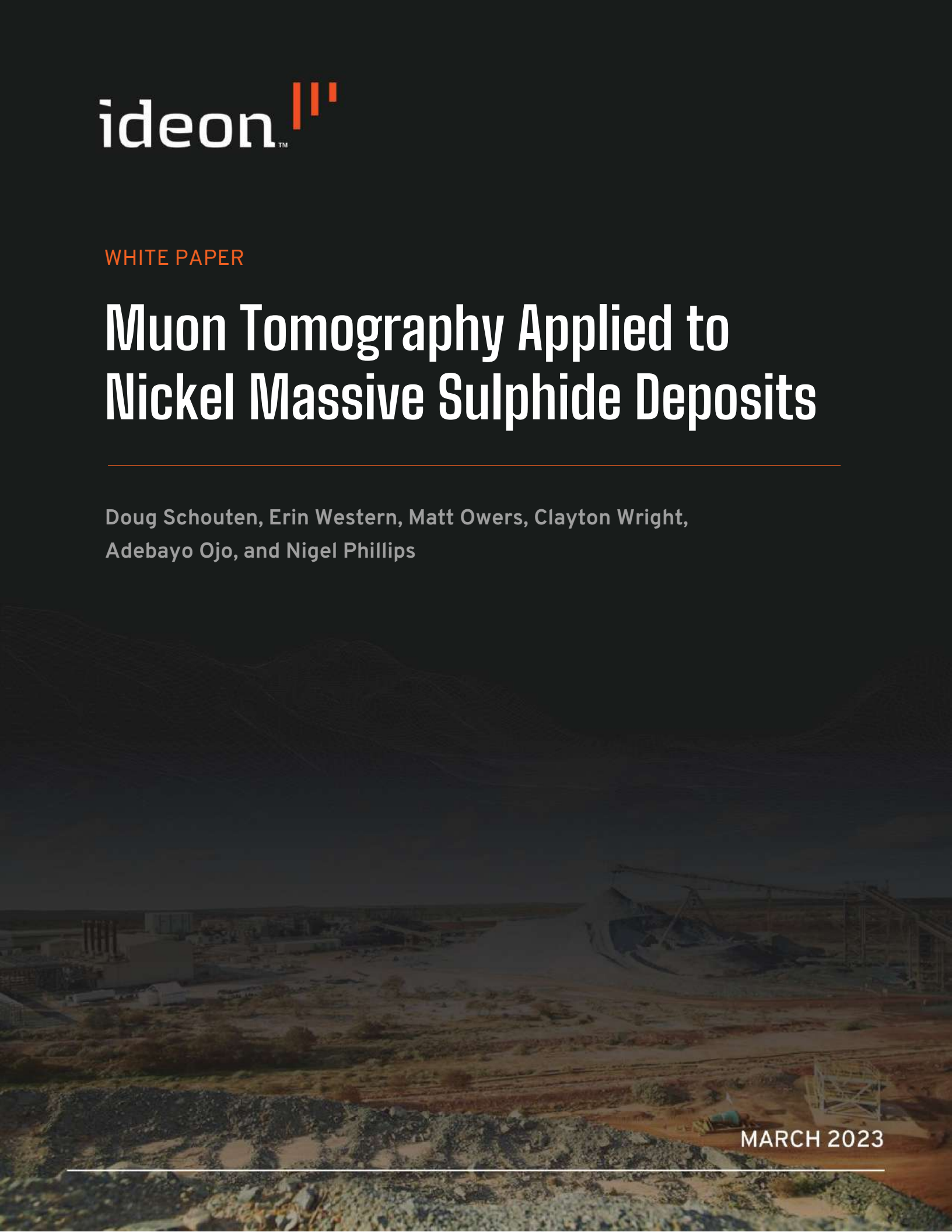

MARCH 2023

Muon Tomography Applied to Nickel Massive Sulphide Deposits

Authors: Doug Schouten[1], Erin Western[2], Matt Owers[3], Clayton Wright[4], Adebayo Ojo[5], and Nigel Phillips[6]

Abstract

Muon tomography is a geophysical method that can provide high-resolution 3D mapping of subsurface density. We describe how this technology was successfully used to image massive sulfide deposits over a 3km strike at two nickel mines in Western Australia, including in a multiphysics analysis that combined ground and airborne gravity datasets with muon tomography using Ideon Technologies' subsurface intelligence platform, in addition to other key insights ranging from regional geological mapping to valuable geotechnical information. The density models were extensively validated by drill information, where that was available.

Introduction

Cliffs and Leinster mines are situated in the Agnew-Wiluna greenstone belt in Western Australia, approximately 150 km apart from each other, and are wholly owned by BHP and operated by BHP's Nickel West group. To elucidate the key findings of the geophysical analysis, we will first describe the geological context of both sites, and also briefly outline how muon tomography works, and in particular how the multiphysics data analysis was performed. We present the outcomes and findings for both sites independently, but the overarching conclusions from both successful projects are summarized at the end.

Geological Context

The Cliffs orebody consists of massive Fe-Ni sulphide mineralization associated with the basal contact of the Cliffs Ultramafic Unit. In the central and northern parts of the Cliffs deposit, the orebody presents as a N-trending, subvertical sheet, approximately 500m wide (down-dip) and plunging gently southward from surface for ~ 1.5km. The massive sulphide portion is typically less than 2m thick but can reach up to 6m in thickness (Perring et. al. 2016).

At the southern end of the Cliffs deposit, the strike of the mineralized basal contact changes from broadly north-south to northwest-southeast. Here the disseminated portion of the orebody is preserved

[1] Ideon Technologies, Inc.
[2] BHP Nickel West
[3] BHP Nickel West
[4] BHP Nickel West
[5] Ideon Technologies, Inc.
[6] Ideon Technologies, Inc.

and reaches up to 30m in thickness. This area is interpreted to be a strain shadow within which disseminated, matrix, and stringer mineralization; spinifex-textured flow tops; and cumulate-textured, serpentinised ultramafic have escaped later stages of deformation (Perring et. al. 2016).

The Cliffs Ultramafic (UCL) has undergone serpentinisation and talc-carbonate alteration resulting in a density of approximately 2.8 g/cc. The Never Can Tell Basalt (NCTB) that forms the stratigraphic footwall to the UCL has a density of approximately 2.85g/cc. The massive FeNiS ore domain has an average density of 4 g/cc. The variability in density between the ore and host rocks at Cliffs, existing underground drives and the well-constrained geological model against which results could be validated, flagged the deposit as the ideal location to trial muon tomography.

At Leinster, the Perseverance Ultramafic Complex (UPC) hosts several Type-1 Fe-Ni sulphide ore bodies including Perseverance, Venus, and Rocky's Reward. Similar to Cliffs, massive FeNiS mineralization is associated with the basal contact of the UPC but is also structurally remobilized in places into the dacitic footwall (Perring et al. 2016). The density of the massive FeNiS ore also differs from the serpentinised ultramafic and felsic host rocks at Leinster. The 2km-long Upper Access drive between Perseverance and Venus provided an ideal location to deploy large, gallery-style muon sensors and effectively screen the volume above the drive for undiscovered massive FeNiS mineralization from readily accessible existing infrastructure.

The Rocky's Reward Ultramafic (URR) Is a structural slice of ultramafic rock immediately west of the UPC that hosts the Rocky's Reward and Harmony ore bodies. Mineralization is associated with distinct terrace structures hypothesized to recur down-dip of the known Rocky's Reward terrace, which is the basis of the Balboa exploration target. Drill testing of the Balboa exploration target was undertaken in 2021 and these drill holes were identified as an opportunity to deploy borehole muon tomography.

Muon Tomography

Muon tomography (D Schouten, 2022) is a geophysical method predicated on measuring the intensity of muons, which are naturally occurring sub-atomic particles arising from supernova explosions in space. Cosmic rays collide with matter in the Earth's upper atmosphere to create muon flux that travels to Earth in straight lines at almost the speed of light. Muons, which pass through the Earth's surface about once/minute for every square cm (J Beringer, 2012), are highly penetrating particles that progressively lose energy at a rate proportional to the density of the material through which they pass. By measuring the directional muon intensity [cm^{-2} s^{-1} sr^{-1}] using muon-tracking detectors placed underground, we can infer the density distribution of the material the muons encountered along their path.

The first recorded use of muon-based geophysics was by E. P. George in the 1950s, who used muon attenuation to measure the average overburden of material above a railway tunnel in Australia. It has since been used to study the internal structure of volcanoes (J Marteau, 2012), in mineral exploration to map ore bodies (D Schouten, 2022), and to detect voids in archaeological site investigations (K Morishima, 2017).

To perform muon tomography, muon-tracking detectors are deployed around the target geological structure to record the trajectory of each muon that passes through them. These detectors are placed at various positions to capture muon trajectories from multiple paths through the region of interest. As exposure time increases, the relative uncertainty of the observed muon intensity from each direction diminishes, and the true underlying structure of average density emerges in the 2D radiographs produced by each detector. By combining data collected from multiple muon detectors deployed at different lateral placements or depths, a 3D density model can be derived.

Muon Detectors

In this case study, two different muon-tracking detectors were used: a large gallery-style detector, and a narrow cylindrical borehole detector. Both detectors have an angular resolution of approximately 25 milliradians, depending slightly on the angle of incidence, and high efficiency (> 90%) for tracking muons that pass through them.

Both detectors are based on scintillator technology, which was selected due to its deployability in regulated mine environments (in contrast to some types of gas mixtures for gas-based particle detectors), its robustness and longevity, and good balance of achievable angular resolution and cost. The properties of the gallery detectors are discussed in greater detail in (D Schouten, 2018). The borehole detectors are 3.5 meters long, 89 millimeters in diameter, and suitable for deployment in uncased HQ holes. In the top sections of the boreholes, through unconsolidated overburden, a suitable casing was installed, to prevent ingress of debris. Multiple borehole detectors were positioned in each of three drillholes at the Balboa exploration target site, connected to one another and to the surface via communications and mechanical cables in a daisy-chain configuration. Data from all detectors was aggregated in a device on the surface before being uploaded for processing via cellular link (see example in Figure 1).

Figure 1 - The surface box (left) and borehole muon detector (right) employed in this case study. The equipment is designed, manufactured, and deployed by Ideon Technologies.

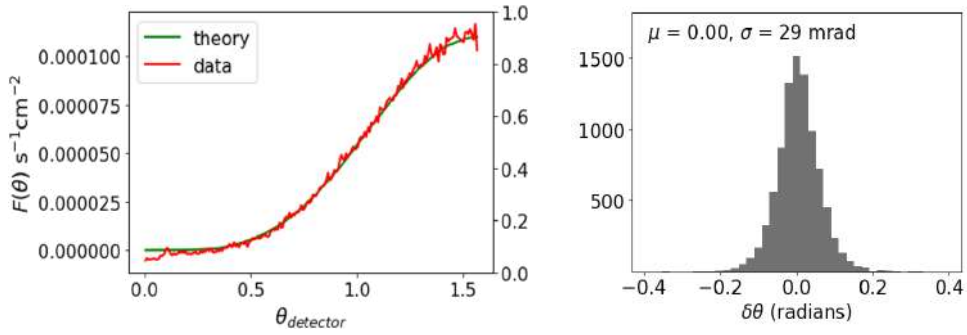

Figure 2 - Performance of the borehole muon detector, seen by comparison of the measured muon flux at sea level (red curve, on the right) compared to the theoretical prediction (underlying green curve, on the right) using the modified Gaisser model **(A Tang, 2006)**. The right distribution shows the residual of measured muon zenith angle for a borehole muon detector compared to an independent measurement with an auxiliary tracker. The inferred angular resolution over all incidence angles from 0° to 50° is 29 milliradians, or approximately 1.6°.

Analysis Methodology

Field data acquired throughout the projects were processed through Ideon's standard data processing algorithms. The expected number of muons N_exp detected within a given pixel p for a solid angle Ω is given by the following equation (D Schouten, 2022 and 2018):

$$N_{exp} = \Delta t \int_{\Omega_p} \left(\int_0^{\infty} D_\mu(E,\theta) \cdot p(E;\mathcal{O}) dE \right) \alpha(\hat{n})\, d\Omega$$

Ideon has developed a robust, precise model that describes the expected intensity of muons at the surface $D_\mu(E,\theta)$ as a function of initial muon energy E and zenith angle θ, using data collected over the past six decades (D Schouten, 2022). The units of intensity are cm^{-2} s^{-1} sr^{-1}. As muons propagate , they lose energy at a rate proportional to thedensity of material they traverse. The probability $p(E;\mathcal{O})$ that a muon penetrates through a length dl of a given density distribution $p(x,y,z)$ is calculated via Monte Carlo simulations. In the equation above, the opacity O, defined as $(\mathcal{O} = \int_{\text{path}} \rho(\text{x},\text{y},\text{z})\ \text{d}\ell\ )$, is multiplied by the muon flux at sea level to determine the muon intensity at any given rock depth. The muon survival probability depends on initial energy; hence, the contribution is summed over all relevant energies. Finally, the detector active area and performance is accounted for in the $\alpha(\hat{n})$ term. The integration is performed over all angles corresponding to a field of view Ω_p above the detector, defined for each pixel p in the radiograph and multiplied by the exposure time Δt.

A geological model is developed based on *a priori* geological information about the rocks and other features in the study area. The statistical comparison of the expected number of muons to those observed in the field reveals high- and low-density with significance correlating with regions of more and less muon attenuation. The statistical significance in each pixel is defined as a Z-score.

$$z = \frac{\mathrm{N} - \mathrm{N}_{exp}}{\sigma_N},$$

where N is the observed number of muons and σ_N is the statistical uncertainty of the expected number, which follows a Poisson distribution. In all the following, the prior geological model consists only of an assumed uniform density ρ_0 in the subsurface, and a digital elevation model taken from airborne LIDAR data.

The expected and observed muon datasets are subsequently inverted into a 3D density model $\rho(x, y, z)$ by minimizing a global function ϕ that incorporates a data misfit term for the muon tomography data and/or other datasets (e.g., ground and airborne gravity) with complementary sensitivities compared to the density model, and a model objective function that ensures model smoothness and that can incorporate optional additional information, such as spatial weighting terms and a reference model:

$$\min_{\rho(x,y,z)} \phi = \min_{\rho(x,y,z)} (\phi_D^{\mu} + \lambda_g \phi_D^{g} + \lambda_{gz} \phi_D^{gz} + \beta \phi_M), \text{ where}$$

$$\phi_D \sim \sum_i \left(z_i - \sum_j G_{ij} \rho_j\right)^2, \text{ and}$$

$$\phi_M \sim \sum_w \alpha_w \int_V \left(\frac{\partial \rho}{\partial w}\right)^{q_w} dV + \alpha_r \int_V \rho^p \, dV$$

where ϕ_D^{μ}, ϕ_D^{g} and ϕ_D^{gz} is data misfit for the muon tomography, ground gravity, and airborne gravity data compared to an initial model, respectively, λ_g and λ_{gz} scales the relative contribution of muon, ground and airborne gravity gradient data in the inversion, β is a trade-off parameter that controls the relative importance of model smoothness and data misfit and ϕ_M is a model objective function that ensures smoothness (K Davis, 2011) (Tarantola, 2005). In the case of muon tomography, G_{ij} is a sparse sensitivity matrix that relates the Z-score of the ith pixel z_i in the radiographic images to the anomalous density ρ_j of the jth voxel in the image volume, α_w is a constant that penalizes roughness in each of the $w = x, y, z$ coordinates and α_r is another constant that penalizes deviations from a reference model. In cases where only muon or gravity data is incorporated into the inversion, the other terms are simply excluded from the objective function.

The 3D density model that is derived is relative to the assumed uniform density – i.e., the absolute density is simply $\rho_{\text{abs}}(x, y, z) = \rho_0 + \rho(x, y, z)$. This is only a calculational tool to ensure the initial model is “close” to the true geology and has no bearing on the final result. The measurement is properly an absolute density measure, without any prior constraints (except where otherwise noted).

Analysis and Results

Data Collection

Cliffs Mine

A muon tomography survey was first carried out at Cliffs Mine. Five gallery-style muon detectors (ID 05 - 09) were deployed in the 362L level at approximately 200m true vertical depth (TVD) with the goal of imaging a known mineralization (see Figure 3) as a demonstration of the technological feasibility. The data collection and analysis were performed "blind", without any reference to the prior geology (except for an assumed uniform density as described above) – which was then revealed once the muon tomography analysis was complete. The primary purpose of this phase was to provide a "standard candle" of the muon tomography technology, to be able to use it with confidence elsewhere in BHP Nickel West's portfolio.

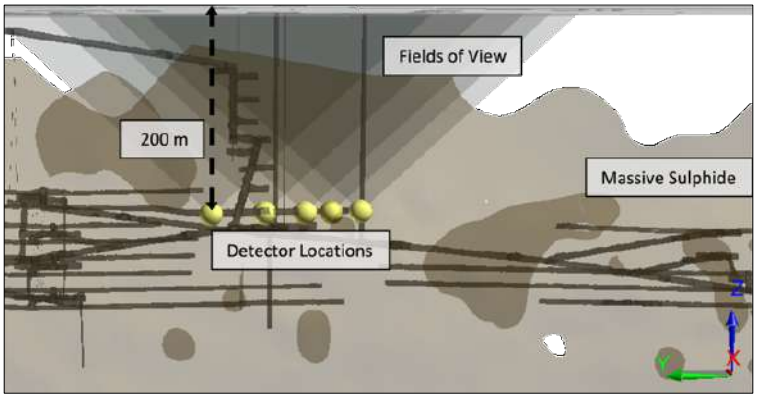

Figure 3 - Survey layout at Cliffs Mine showing detector locations, fields of view, and target mineralization. The fields of view are pyramidal cones with opening angle 120° from each detector location. The sub-vertical massive sulphide lens is partially imaged.

Leinster Mine

After successful completion of the Cliffs mine project, the Leinster project proceeded in three phases:

- In Phase 1 and 2, gallery detectors collected data at nine locations along an underground drive that connected mining operations for the Perseverance and Venus deposits, at vertical depths of approximately 800m; and
- In Phase 3, borehole detectors were installed to the north to explore the Balboa exploration target zone at downhole depths ranging from 200 to 400m.

The goals of the project were twofold: first, to image the potential continuity in between the Perseverance and Venus massive sulfide deposits, and second, to search for evidence of additional massive sulfide mineralization proximal to the Rocky's Reward terrace.

Additionally, BHP had already acquired a rich dataset of downhole density and lithology data, as well as both ground and airborne gravity datasets. The Ideon subsurface intelligence platform was employed to perform a multiphysics analysis, comprising muon tomography, gravity (ground and airborne), and drill data. Important insights and complementarities between the data were uncovered in this analysis, as are explained in Figure 5 below.

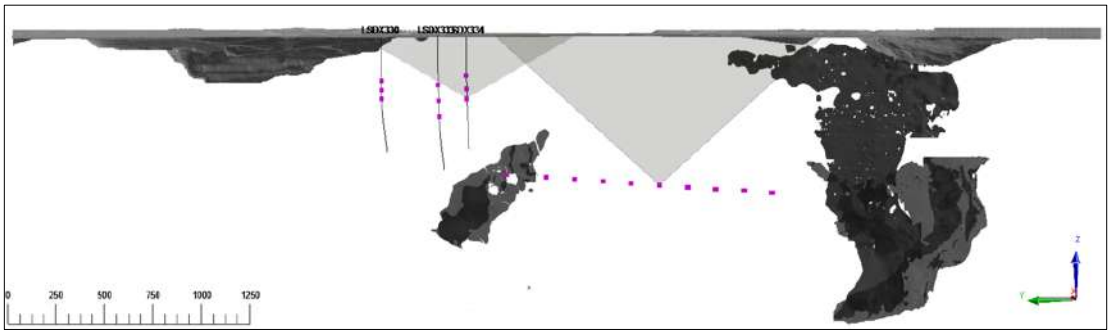

Figure 4 - Survey layout at Leinster Mine showing gallery and borehole detector locations, two example fields of view, and existing mineralization (Venus on the left, Perseverance on the right). The strike length explored in the survey was larger than 2.5km.

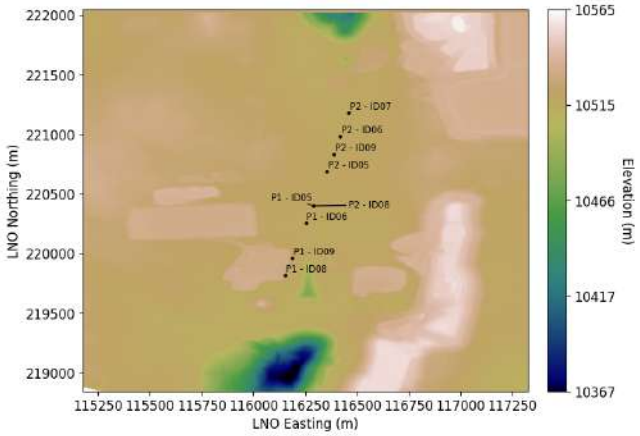

Figure 5 - Plan view of the Leinster survey gallery detector locations. Note how ID05 and ID08 detectors from Phase I and Phase 2 are in the same location.

Data Quality

In both the Cliffs and Leinster deployments, detectors were commissioned and operated first on the surface to ensure functionality and validate expected muon flux measurements above ground, before being maneuvered into place underground.

The data retrieved from gallery detectors was assessed for (a) continuity on a per-channel basis for each detector, (b) compatibility between detectors, and (c) compatibility with simulations. To establish uniform performance over time, a Durbin-Watson test statistic was calculated from the time series data. Channel response, various voltage and current measurements in the detector electronics, and muon rates recorded by the detectors were uniform and within normal parameters for data collected in the survey.

Data Analysis

Cliffs Mine

After 1 ½ months of data collection, highly significant density anomalies were identified ($p < 10^{-10}$), as shown in Figure 6. The data were inverted following the L_2-normed inversion methodology described above and in (D Schouten, 2018) and (D Schouten, 2022), yielding a density model discretized into 5m x 5m x 5m (125 m^3) voxels. BHP then provided the detailed drill data acquired during exploration and mine operation phases, provided as a kriged density block model. Comparison of the drill data and the muon tomography inversion yielded very good correspondence, as shown in Figure 7.

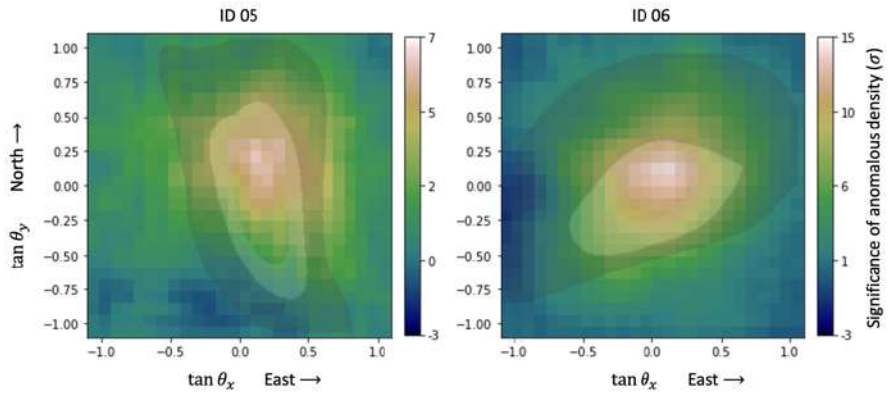

Figure 6 – Maps of the significance of anomalous density, z, from two of the detector locations. The colour scale indicates the significance, in units of standard deviation (assuming a Gaussian distribution of the data measure). The overlain transparency layer shows two contour levels of the same from forward simulation of a simplified massive sulphide lens within the survey area.

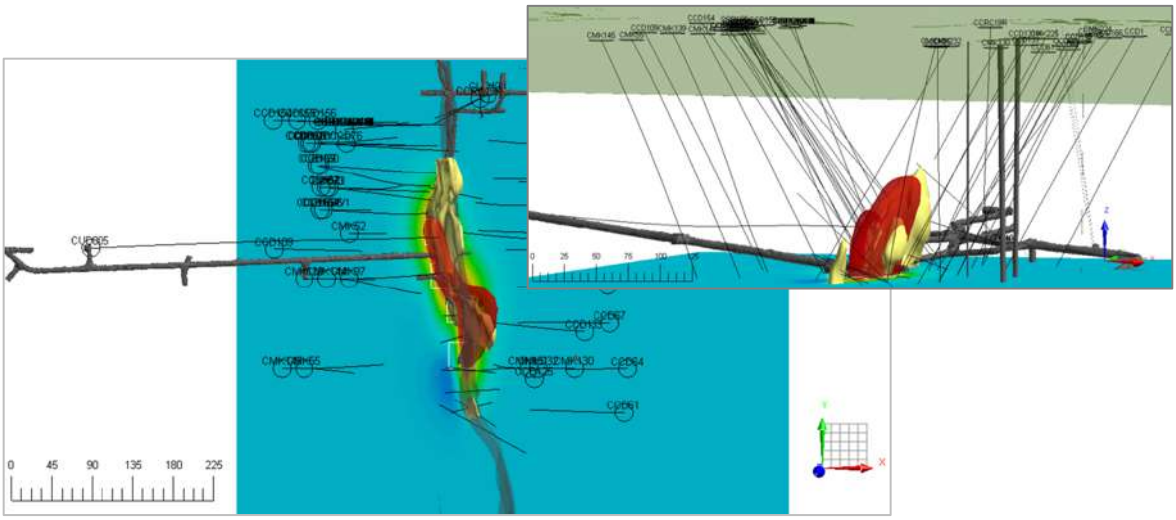

Figure 7 - Resultant 3D density model from muon tomography, compared to the drillhole analysis. On the left is shown a plan view, with a horizontal section of the density model from muon tomography. Also shown is an iso-surface corresponding to > 3.0 g/cc density (red surface) from the muon tomography, in comparison to the interpolated density model from drill data (yellow). The inset image shows a view looking to the northwest of the same section and density iso-surfaces, in relation to the drillholes used to map the deposit in the survey region.

At the Cliffs Mine, muon tomography recovered a detailed density model that coincided with the known massive and disseminated mineralization with few-metre spatial resolution. This was an important positive field demonstration of the efficacy of muon tomography for this mineralization type and geology, and provided BHP the assurance that the method could be used in exploration and resource-mapping applications.

Additionally, the top profile of the mineralization was indicated in the muon tomography inversion (see Figure 8), and the enhancement of the lobe of high density towards the Easting direction (see red iso-surface in Figure 7) provided evidence for extension of the mineralization, in an area where the local drill density was more sparse.

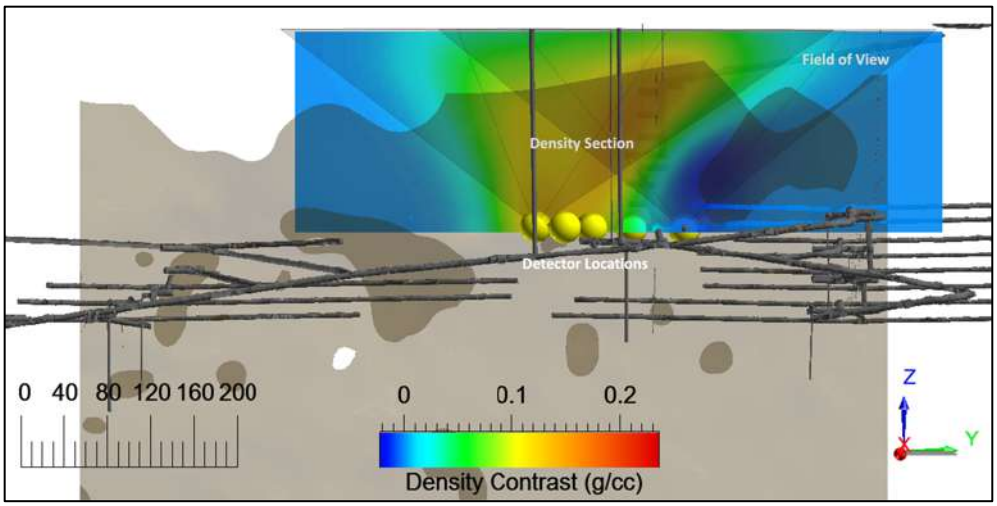

Figure 8 - North-South section of the unconstrained inverse density model from muon tomography data. A key finding in these results was the ability for the muon tomography data to map the weathered profile of the massive sulphide, which was characterized by a density contrast between weathered overburden and the fresh rock at approximately 60m depth.

Leinster Mine

The same data processing steps were applied to the Leinster data for the gallery detectors, as in the Cliffs project. Data that failed quality criteria were excluded from the analysis, which in this case consisted of a partial set from ID 07, ultimately due to a failed power converter. For the borehole detectors in Phase 3, analogous data processing steps were applied, though of course the muon trajectory determination was different due to the cylindrical geometry.

Interesting density variations were observed in both Phase I and 2 data, as shown in Figure 9. The density variations were also highly statistically significant, as shown in Figure 10. What can be seen immediately is evidence for a North-trending high-density structure with a clear delineation from the country rock (with density ρ_0 = 2.7 g/cc). There are also subtler lower-density features to the East seen in some of the data. These are interpreted very clearly in the 3D density reconstruction below.

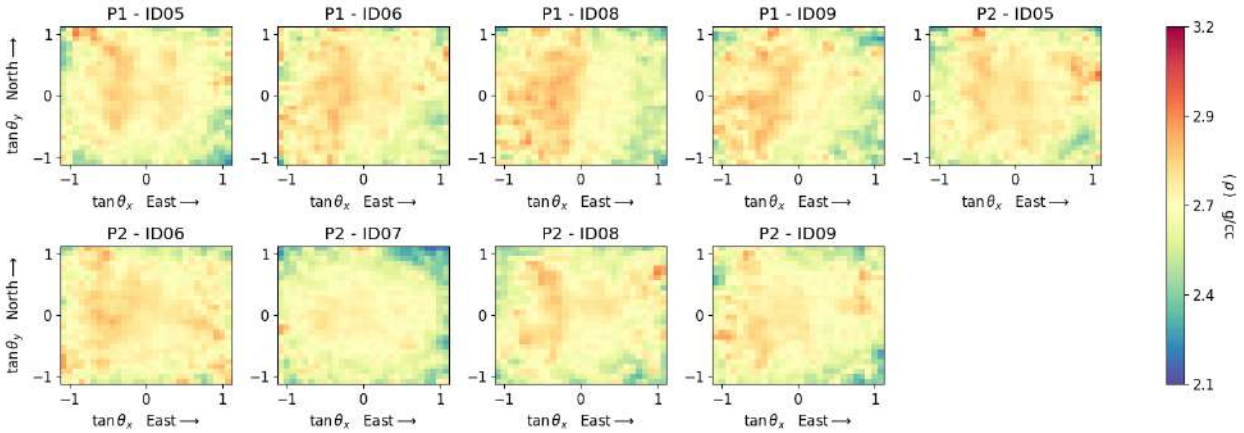

Figure 9 - Average density measurements, in bins of dimension $\tan\theta$ = 0.080, for Phase I and Phase 2 detector data. High average density bands are observed in the West. In detector ID 07 data, there is a significant low-density anomaly observed to the NorthEast direction – which was identified after the survey was completed as due to voids from mining operations around the Venus deposit.

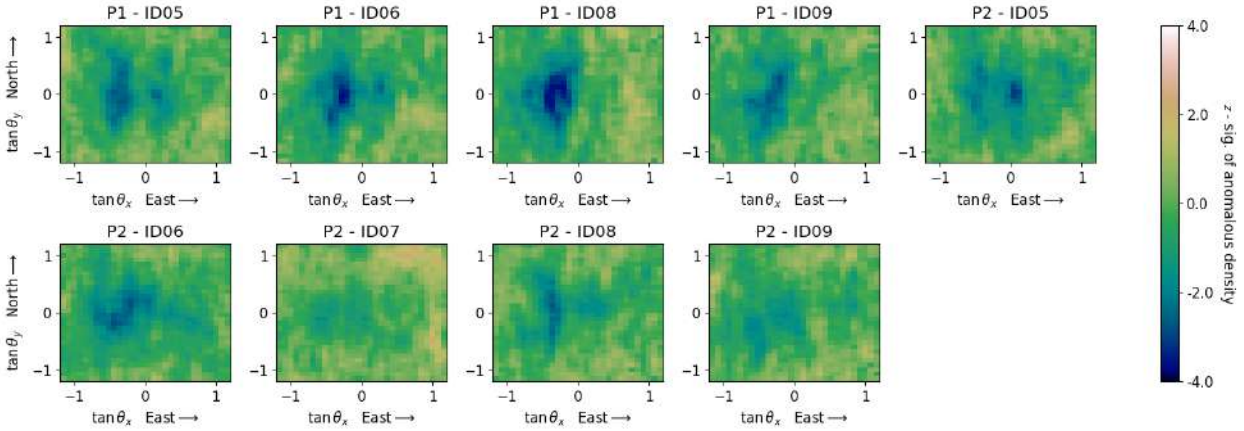

Figure 10 - Significance of anomalous average density (z) measurements seen in the detector data in Phase I and 2. The p-value is < 10-6 for accepting the null (uniform density) hypothesis. Note the similarity in P2 – ID 08 and P1 ID 05, which are data taken from different detectors in approximately the same location and at different times. The low-density structure seen from P2 ID 07 data is also highly significant.

Density Inversion

The radiographic images from Phase I and 2 data were incorporated into a 3D density reconstruction, using the methods described above. No geological constraints were applied in the inversion (specifically, $\alpha_r = 0$). The resultant inverse model revealed very good insights about the subsurface geology. Looking at a horizontal section of the density model at the surface, we can see that the subtle low-density features seen in many of the radiographs are arising from stockpiles at surface. It is worth highlighting that the stockpile perimeters are mapped with 10m accuracy from muon detectors

more than 800m away. Additional density variations can also be seen, which are vertical extensions of deeper structures.

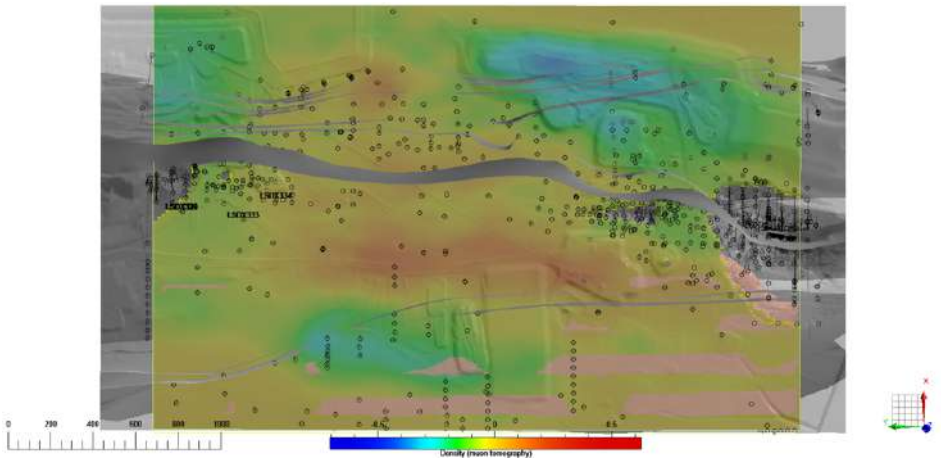

Figure 11 - Shallow horizontal section of inverse density model, derived from muon tomography data in Leinster Phase I and Phase 2. The surface topography and main geological contacts, as well as drillhole collars, are shown in greyscale. The high density of drilling in the North and South extents of the survey area are proximal to the Venus and Perseverance deposits.

The inverse model was incorporated into the prior geological model to generate an alternative set of synthetic muon data. Comparison of these data to the null geological model with uniform background density is shown in the z radiographs shown in Figure 12.

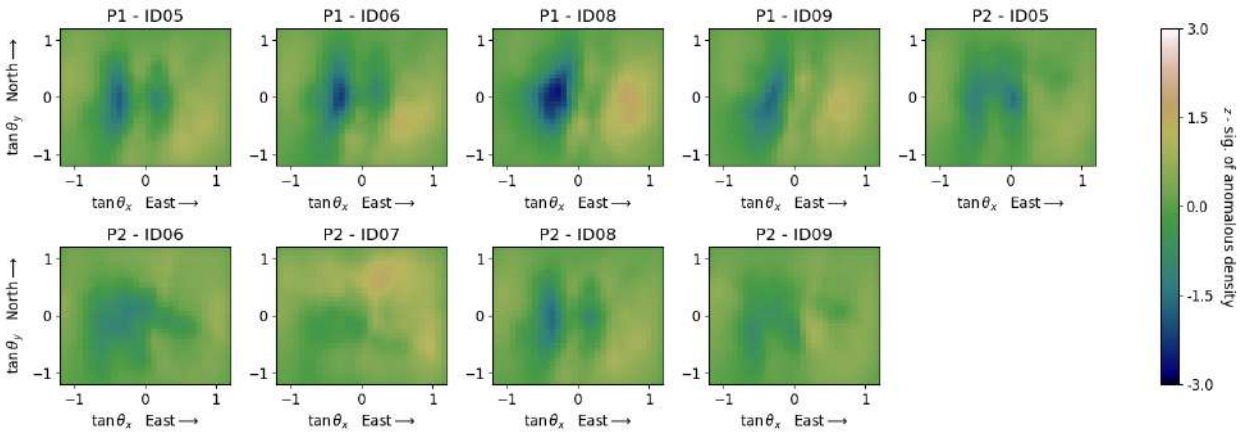

Figure 12 - Significance of anomalous density in synthetic data taken from forward simulation of the inverse density model, compared to the uniform prior geological model. Comparison to the field data shows that the inverse model is capturing the density features well, and the residuals are small.

Comparison to drill data

Extensive drill data was available from the survey area, albeit with large spatial gaps between the Venus and Perseverance deposits. The density assays from all the analyzed drill core were leveraged in an ordinary kriging interpolation to define an alternative "reference" geological model. The field data was compared to a forward simulation of the reference model, and the resultant z radiographs are shown in Figure 13. The compatibility with the muon tomography data is improved (compared to the uniform geological model in Figure 10), however there remain significant variations. This is not surprising, given the large areas with sparse drilling data.

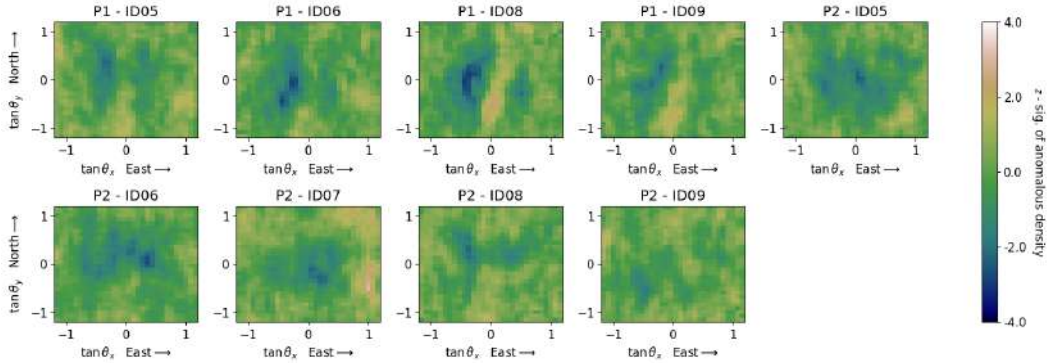

Figure 13 – maps of z in which N_{exp} is calculated using a geological model with density values set from kriging interpolation of the drill density assay measurements. This model is in better accordance with the data compared to the uniform density model, although significant anomalies remain unaccounted for.

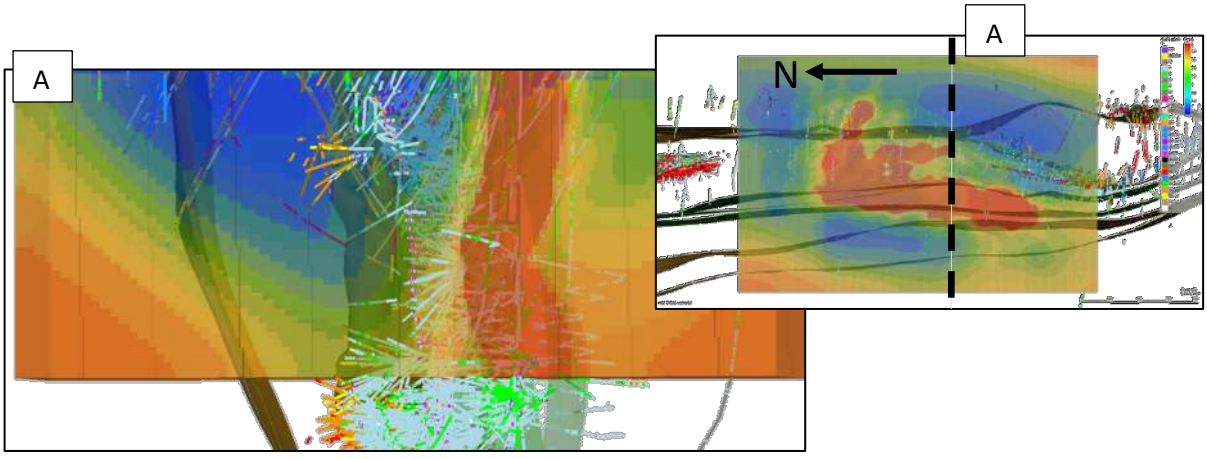

Figure 14 – Vertical section of the unconstrained muon tomography inversion. The location of the section is indicated in the inset. There is very high-resolution correspondence with the model and the sub-vertical mafic unit in this area, where there is a high density of drill data to inform the geological model.

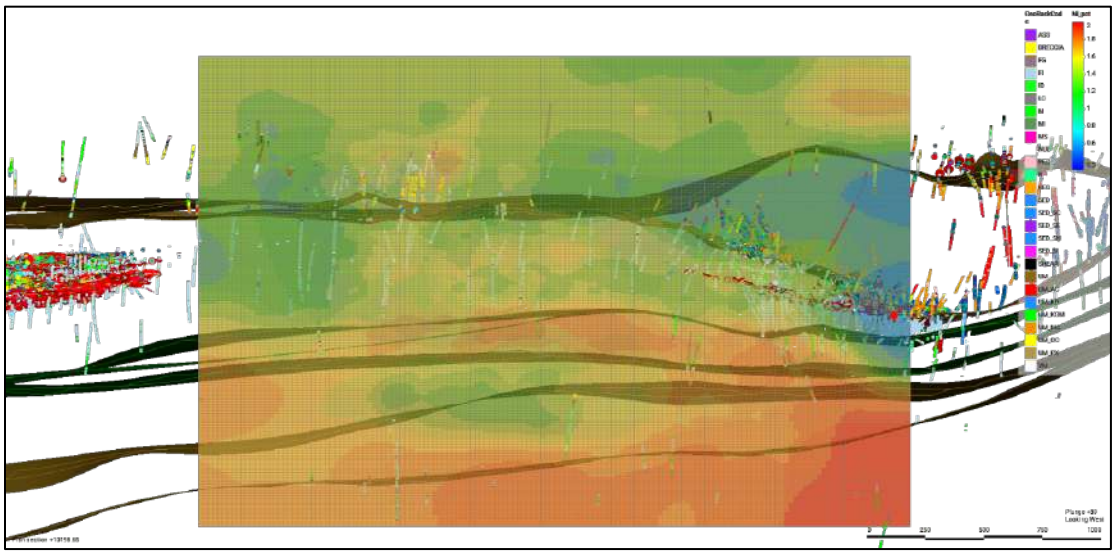

Figure 15 – Horizontal section of the muon tomography inverse model at 200m depth. The sub-vertical mafic unit defined by two geological contacts is confirmed by the muon tomography model with good resolution.

Additional features were found in the muon tomography density model that had very good correspondence to geological features that were validated in the drilling. First, a massive sulphide to the East, at the Northern extent of the survey, was isolated as a high-density structure in the inverse model, as shown in Figure 16.

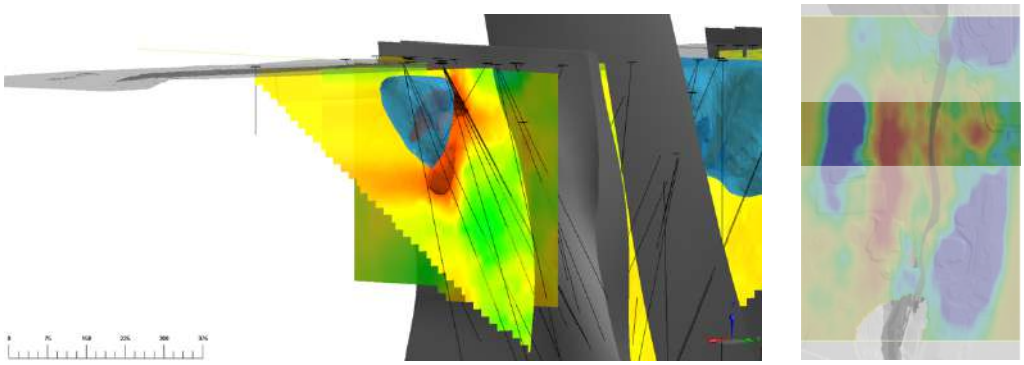

Figure 16 (Left) – massive sulphide structure, revealed in drill data and shown in the interpolated density model derived from drilling with East-West and North-South slices shown along with a red iso-surface corresponding to > 3.5 g/cc. The density anomaly seen in the muon tomography data is shown by the semi-transparent blue iso-surface corresponding to a 0.3 g/cc anomaly. The massive sulphide was mapped from > 750m away by the muon detectors. (Right) – a plan view of the survey showing the density model at -50m TVD, with the slice corresponding to the left view highlighted. The massive sulphide is clearly seen adjacent to the North-South trend proximal to the HW-Shear contact.

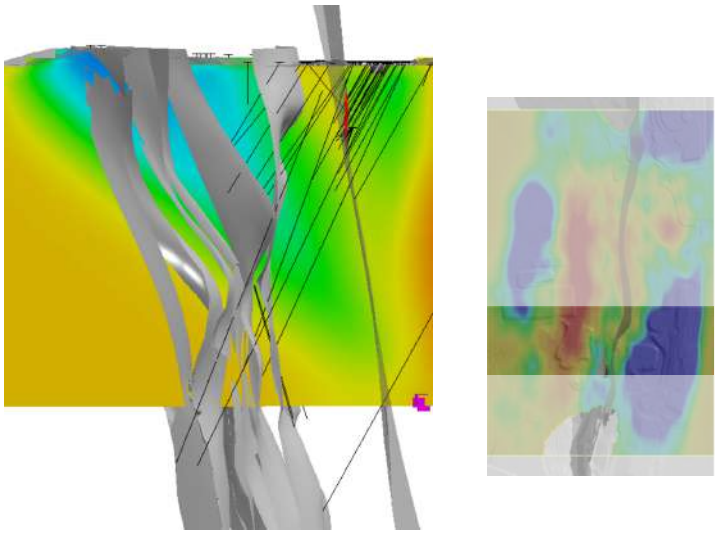

Figure 17 (Left) – the edge of the Perseverance deposit, seen as the narrow red band near surface, with a section of the muon tomography density model. The sub-vertical high-density feature maps very well to the deposit and the HW-Shear contact, where (massive) sulphide is remobilized. (Right) – a plan view of the survey showing the density model at -50m TVD, with the slice corresponding to the left view highlighted.

Multiphysics Joint Inversion

Airborne gravity gradient and ground gravity data acquired by BHP were incorporated along with muon tomography data into the subsurface analysis in a multiphysics joint inversion. Visual inspection of the airborne gravity data indicated interesting complementary features to the shallow section of the

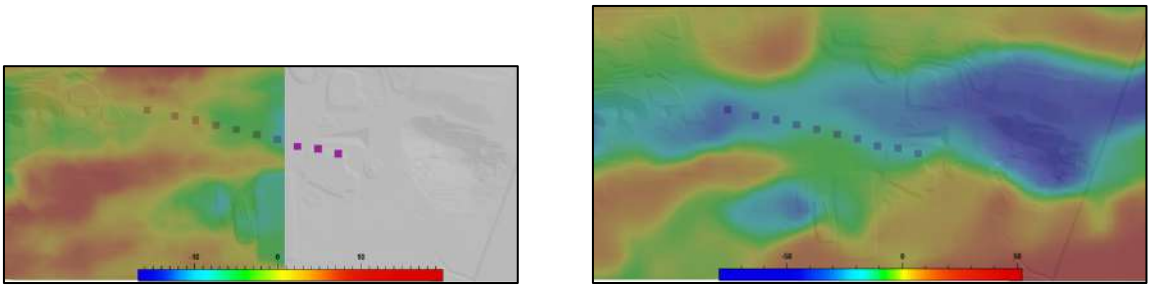

Figure 6 (Left) the Bouguer anomaly (gz) for ground gravity survey, after applying a linear regional trend extraction method and (Right) the vertical gradient (gzz) for airborne gravity survey, also after application of a regional trend correction. The units are mGal (left) and Eotvos (right). Comparison between the gravity data and the muon tomography density reconstruction shows broad compatibility.

muon tomography density model seen in Figure 11. It has been shown that muon tomography provides

superior spatial and density resolution compared to ground gravity (K Jourde, 2015) when the configuration of the muon tomography survey is optimal from a geometry perspective. Given the survey configuration with all the detectors in Phase I and 2 located on approximately the same depth plane, it was expected that the gravity data, which is most sensitive to near-surface features, could provide additional depth constraints in a joint inversion.

In the joint inversion, the relative model weights were set with $\lambda_g, \lambda_{gz} = 1$ and for both ground and airborne gravity gradient, a model weighting was applied based on distance from the gravity station locations (D Oldenburg, 1998), according to $d^{\frac{3}{2}}$. The data were pre-processed with terrain corrections assuming a host rock density of 2.67 g/cc, and a regional trend was extracted from the data using a linear regression. The resultant anomalous gravity (gradient) readings, interpolated over their respective domains is shown in20. Iso-surfaces of density from the muon tomography and joint inversions are shown in a detailed section view in Figure Figure 7.

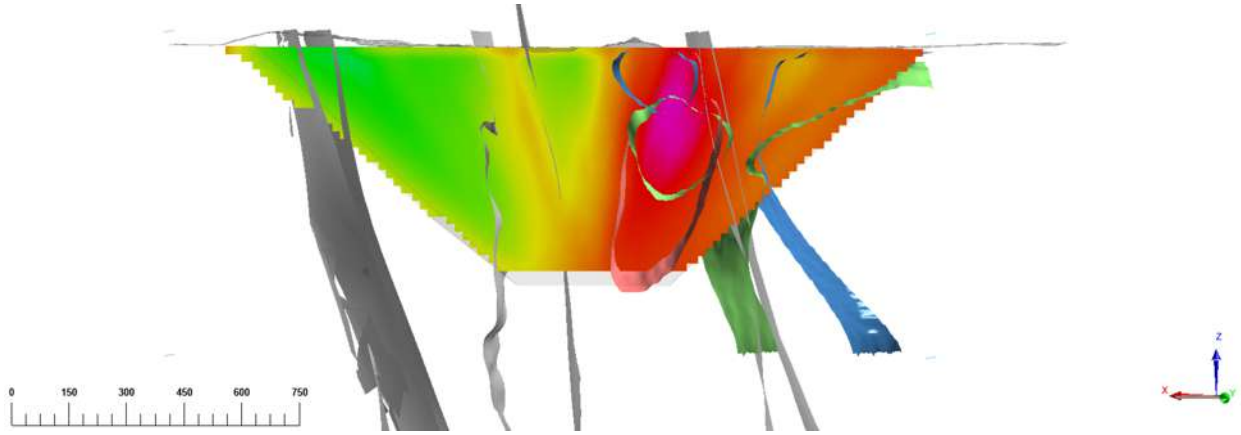

Figure 7 - Section of the joint density inversion. The slice shows the density profile in the muon tomography model, and the iso-surfaces from muon tomography (red), gravity (blue) and joint (green) inverse models. The narrow feature proximal to the Perseverance deposit and HW-Shear was not seen in the gravity data, presumably due to its intrinsically lower resolution. A subtle low-density feature seen in the gravity data (leading to a slight depression in the iso-surface to the West) was also seen as a near-surface structure by the muon tomography data, from a distance of > 750m to the nearest detector.

Borehole Muon Tomography

In Phase 3 of the project, Ideon borehole muon tomography detectors were deployed in three holes adjacent to the Rocky's Reward terrace, to investigate whether any high-density features consistent with massive sulphide mineralization existed within a target region that was hypothesized to be prospective under a geological hypothesis, with indications of enhanced conductivity from an electro-magnetic (EM) survey. A total of nine borehole detectors were installed in three holes along approximately 500m, to the

North of the Phase I and 2 gallery locations, between 200 and 400m TVD. The detectors were powered by a small solar array installation at the surface and connected to the Ideon cloud via a 4G LTE network.

Data collection was interrupted a few times due to storms that disrupted solar power provision, but otherwise no significant data quality issues were seen. A combined density model was derived by inverting the muon tomography data from Phase I, 2 and 3. It is noteworthy that, in contrast to other geophysical techniques, data from disjoint and overlapping periods and detector locations can be combined easily to incrementally enlarge a study area and improve resolution capability.

A shallow section of the density model is shown in Figure 89. The main geological features are seen in agreement between the Phase I and 2 gallery survey and the borehole survey in Phase 3. This shallow section also agrees well with the anomalous airborne gravity gradient shown in **Error! Reference source not found.**. A higher-density feature seen in LSDX330 is seen as a shallow anomaly in the 3D density inversion, a vertical section of which is shown in Figure 10.

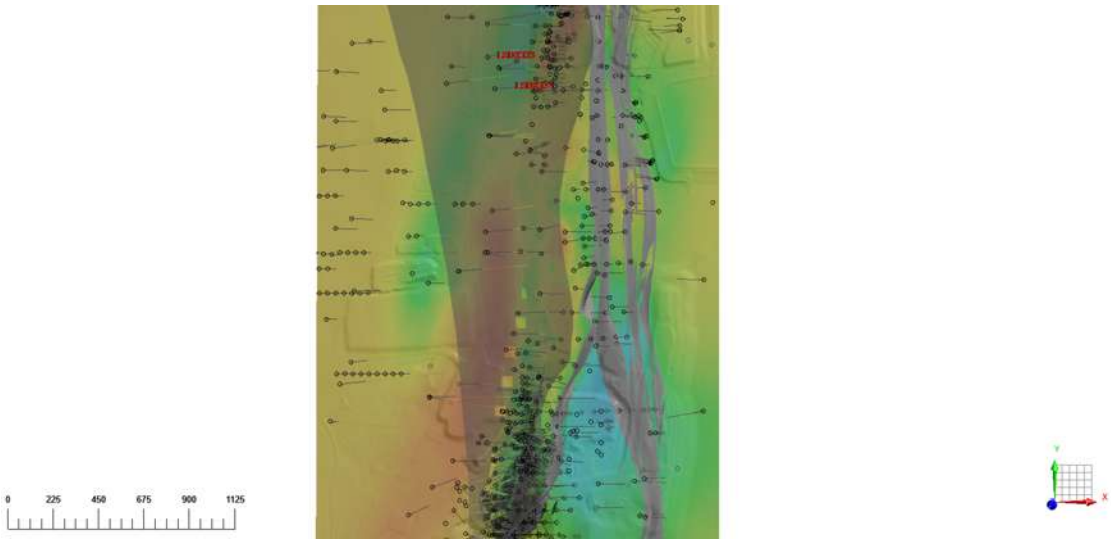

Figure 8 - Shallow section (100m) of the unconstrained inverse density model from Phase I, 2 and 3 muon tomography data at Leinster Mine. The main geological features are seen in as largely continuous between the Phase I and 2 gallery survey and the borehole survey in Phase 3. The borehole collar locations are highlighted with red, and the many other drill holes near the Venus and Perseverance deposits are also indicated. This shallow section also agrees well with the anomalous airborne gravity gradient shown in **Error! Reference source not found.**.

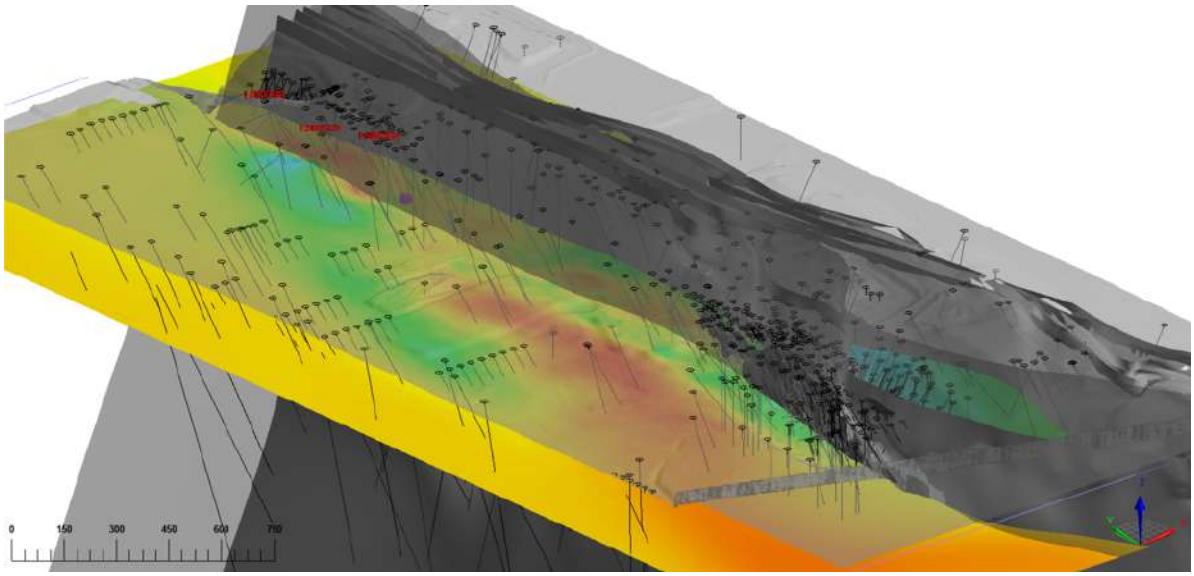

Figure 9 – The same shallow section of the combined Phase I,2 and 3 density inversion as in Figure 84, looking towards the North-East.

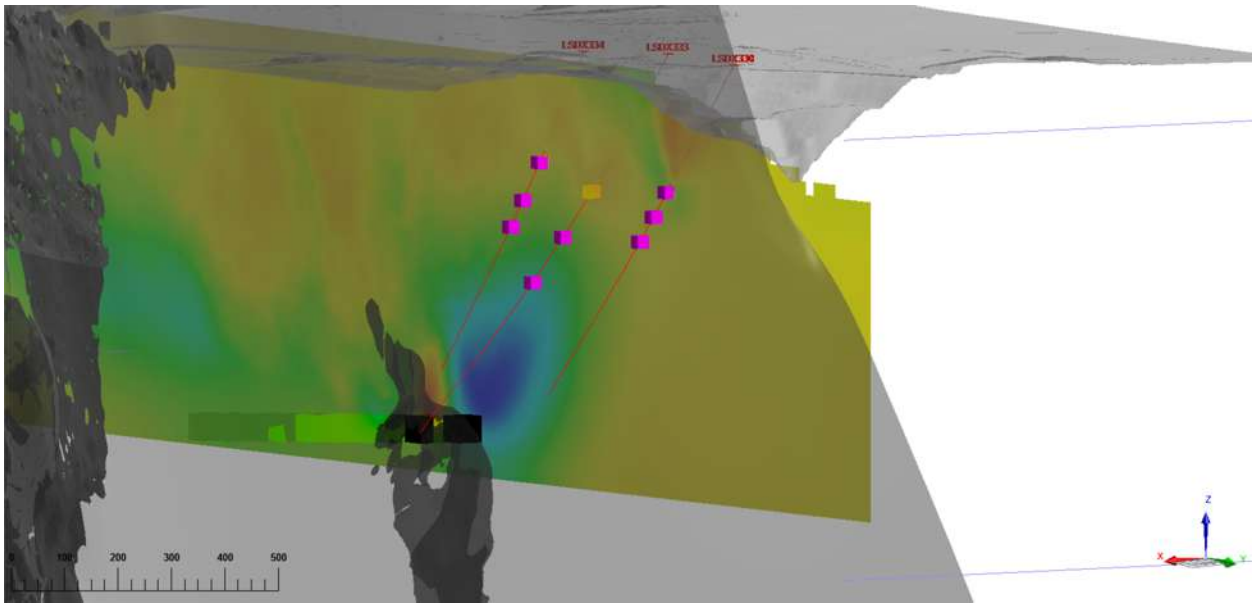

Figure 10 – Vertical section of the joint 3D density model. The locations of the borehole detectors are indicated, and the gallery detector locations are mostly obscured by the section shown. The high-density anomaly near surface proximal to the LSDX330 borehole has not been investigated yet. A discussion of the strong low-density anomaly adjacent to the Venus deposit and below the borehole survey, is discussed further elsewhere.

Outcomes and Findings

Cliffs Mine

A fast muon tomography program at the Cliffs Mine demonstrated the efficacy of muon tomography for detailed mapping of a massive sulphide-hosted mineral resource. Lateral resolution of a few metres, and the ability to locate the boundary of weathered and fresh rock, was demonstrated by comparison to drill data. Evidence for additional mineralization in an extension to a lobe of the nickel ore body was provided from an unconstrained 3D density inversion of the muon tomography data.

Leinster Mine

A wide-area multiphysics analysis of the Leinster area has been performed, integrating

- Ground and airborne gravity data;
- Muon tomography data from > 800m depth, and incorporating the world's second borehole muon tomography survey; and
- Detailed drill assay data,

And yielding many important findings. Importantly, the geophysics data were not constrained by prior geological hypothesis or drill data (except where expressly noted). The data were mutually confirming, and ground truth (drill data) was able to establish the veracity of many density features seen in the muon tomography data. The resolution of the gallery muon tomography was especially good in the lateral (x, y) coordinates, and integration with gravity and drill data provided improved depth resolution, especially near surface. Some key findings included the following:

- Well-known surficial features were mapped with few-metre lateral resolution from muon detectors many hundreds of metres away, providing intrinsic confirmation of the validity of the density model.
- The ability to map relatively small regions of massive sulphide, from detectors installed more than 750m away, was demonstrated.
- Voids from mining activity around the Venus deposit were clearly seen in the inverse models and in the 2D density images from one of the detectors that had this region within its field of view. This demonstrated the geotechnical potential for the technology.
- The regional geology was mapped with very good resolution from a very sparse detector density, and with almost no ground disturbance or minimal operational overhead on the mine.
- Borehole muon tomography was successfully used in a search for massive sulphide mineralization. At the time of this publication, high-density features that were identified have

not yet been investigated with further drilling. Nevertheless, the data was complementary and mutually consistent with data collected from underground gallery detectors and drill data.

- A complex multiphysics analysis using Ideon's subsurface intelligence platform was completed. The complementarity of the gravity and muon tomography datasets added confidence to the inferred density models, and the superior depth penetration and lateral resolution of the muon tomography data drove improved interpretation of the gravity data.

Further work to combine a very high-resolution magnetic dataset, and future drillhole information, is ongoing and may be the subject of another publication.

Conclusions

The case studies at Cliffs and Leinster demonstrated the ability to map subtle details within large volumes of rock, cost effectively, and with very little background information. We were successful in demonstrating the efficacy of muon tomography for

1. Mineral exploration;
2. Resource mapping; and
3. Geotechnical void detection,

and the cost-effectiveness and resolution of such over a wide survey area extending beyond 3km in strike extent and more than 1×10^9 m^3 of the subsurface.

Muon tomography has the power to inform decision-making at earlier stages of exploration and resource definition by fast-tracking the understanding of subsurface geology. Understanding the volume of a prospective lithological unit in the early stages of exploring a new terrane or having an indication of the extents of newly discovered mineralisation has the potential to reduce drilling volume, surface footprint and cost.

Key to its successful application is designing drill holes or underground development for muon tomography. Since the sensors "look" up they are best installed in drill holes or drives located lower than an area of interest. This may be how the method is best exploited in the future but as demonstrated in this case study, deploying muon sensors in existing underground infrastructure has provided abundant information that will be incorporated into ongoing exploration at Nickel West's underground operations.

Bibliography

J Marteau D Gibert, N Lesparre, F Nicollin, P Noli, F Giacoppo Muons tomography applied to geosciences and volcanology [Journal] // Nuclear Instruments and Methods in Physics Research Section A: Accelerators, Spectrometers, Detectors and Associated Equipment. - 2012. - pp. 23-28.

K Morishima et al Discovery of a big void in Khufu's Pyramid by observation of cosmic-ray muons [Journal] // Nature. - 2017. - pp. 386-390.

D Schouten D Furseth, J van Nieuwkoop Muon tomography for underground resources. [Book Section] // Muography: Exploring Earth's Subsurface with Elementary Particles / book auth. László Oláh Hiroyuki K. M. Tanaka, Dezső Varga. - [s.l.] : American Geophysical Union, 2022.

D Schouten P Ledru Muon Tomography Applied to a Dense Uranium Deposit at the McArthur River Mine [Journal] // Journal of Geophysical Research: Solid Earth. - 2018. - pp. 8637-8652.

A Tang G Horton-Smith, V Kudryatsev, A Tonazzo Muon simulations for Super-Kamiokande, KamLAND, and CHOOZ [Journal]. - [s.l.] : Physical Review D, 2006. - 5 : Vol. 74.

K Jourde D Gibert, J Marteau Joint inversion of muon tomography and gravimetry - a resolving kernel approach [Journal]. - [s.l.] : Geoscientific Instrumentation, Methods and Data Systems Discussions, 2015. - 1 : Vol. 5.

K Davis D Oldenburg, V Kaminski, D Bryman, J Bueno, Z Liu Joint 3D inversion of muon tomography and gravity data [Conference] // International Workshop on Gravity, Electrical & Magnetic Methods and Their Applications. - Beijing, China : SEG, 2011.

D Oldenburg Y Li 3-D inversion of gravity data [Journal]. - [s.l.] : Geophysics, 1998. - 1 : Vol. 63.

Tarantola A Inverse Problem Theory and Methods for Model Parameter Estimation [Book]. - [s.l.] : SIAM, 2005.

J Beringer et al Review of Particle Physics [Journal]. - [s.l.] : Physical Review D, 2012. - 1 : Vol. 86.